Environmental Science & Technology

Article

pubs.acs.org/est

Environmental Photochemistry of Altrenogest: Photoisomerization to a Bioactive Product with Increased Environmental Persistence via Reversible Photohydration

Kristine H. Wammer,[*,†] Kyler C. Anderson,[†] Paul R. Erickson,[‡] Sarah Kliegman,[‡,◆] Marianna E. Moffatt,[†] Stephanie M. Berg,[†] Jackie A. Heitzman,[§] Nicholas C. Pflug,[∥] Kristopher McNeill,[‡] Dalma Martinovic-Weigelt,[§] Ruben Abagyan,[⊥] David M. Cwiertny,[#] and Edward P. Kolodziej[▽,○]

[†]Department of Chemistry, University of St. Thomas, St. Paul, Minnesota 55105, United States

[‡]Institute of Biogeochemistry and Pollutant Dynamics, ETH Zürich, CH-8092 Zürich, Switzerland

[§]Department of Biology, University of St. Thomas, St. Paul, Minnesota 55105, United States

[∥]Department of Chemistry, University of Iowa, Iowa City, Iowa 52242, United States

[⊥]Skaggs School of Pharmacy and Pharmaceutical Sciences, University of California, San Diego, 9500 Gilman, La Jolla, California 92093-0747, United States

[#]Department of Civil and Environmental Engineering, University of Iowa, Iowa City, Iowa 52242, United States

[▽]Interdisciplinary Arts and Sciences, University of Washington, Tacoma, Tacoma, Washington 98402 United States

[○]Department of Civil and Environmental Engineering, University of Washington, Seattle, Washington 98195-2700 United States

Supporting Information

ABSTRACT: Despite its wide use as a veterinary pharmaceutical, environmental fate data is lacking for altrenogest, a potent synthetic progestin. Here, it is reported that direct photolysis of altrenogest under environmentally relevant conditions was extremely efficient and rapid (half-life ~25 s). Photolysis rates (observed rate constant k_{obs} = 2.7 ± 0.2 × 10^{-2} s^{-1}) were unaffected by changes in pH or temperature but were sensitive to oxygen concentrations (N_2-saturated k_{obs} = 9.10 ± 0.32 × 10^{-2} s^{-1}; O_2-saturated k_{obs} = 1.38 ± 0.11 × 10^{-2} s^{-1}). The primary photoproduct was identified as an isomer formed via an internal 2 + 2 cycloaddition reaction; the triplet lifetime (8.4 ± 0.2 μs) and rate constant (8 × 10^4 s^{-1}) of this reaction were measured using transient absorption spectroscopy. Subsequent characterization determined that this primary cycloaddition photoproduct undergoes photohydration. The resultant photostable secondary photoproducts are subject to thermal dehydration in dark conditions, leading to reversion to the primary cycloaddition photoproduct on a time scale of hours to days, with the photohydration and dehydration repeatable over several light/dark cycles. This dehydration reaction occurs more rapidly at higher temperatures and is also accelerated at both high and low pH values. In vitro androgen receptor (AR)-dependent gene transcriptional activation cell assays and in silico nuclear hormone receptor screening revealed that certain photoproducts retain significant androgenic activity, which has implications for exposure risks associated with the presence and cycling of altrenogest and its photoproducts in the environment.

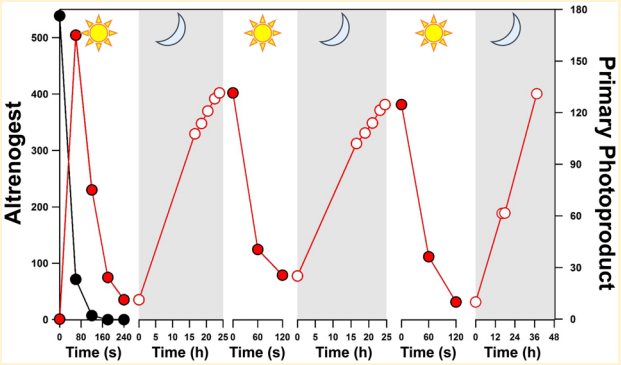

INTRODUCTION

The endocrine disrupting potential of synthetic progestins is of growing concern.[1−3] For example, exposure to levonorgestrel, a human contraceptive, at only 0.8 ng/L reduces fecundity in fish.[1] Because their reproductive effects are observed at subng/L concentrations, a recent review went so far as to state that synthetic progestins may be the pharmaceutical class of greatest concern after ethinyl estradiol.[3]

Altrenogest (ALT, 17-α-allyl-17-β-hydroxyestra-4,9,11-trien-3-one), also known as allyl-trenbolone or ally trenbolone, is a potent synthetic progestin used as an equine and swine veterinary pharmaceutical. Marketed commercially under various trade names including Matrix (for swine), Regu-Mate, and Altresyn (for horses), ALT is administered orally or in animal feed to maintain pregnancy, synchronize estrus for breeding, or postpone estrus after weaning.[4−6] For estrous

Received: May 24, 2016
Accepted: June 29, 2016
Published: June 29, 2016

DOI: 10.1021/acs.est.6b02608
Environ. Sci. Technol. 2016, 50, 7480−7488

synchronization, swine receive 210−360 mg doses of ALT over 12−18 days, while in horses 230−400 mg is used over 15 days.[7,8] For pregnancy maintenance in horses, an additional 3000−6000 mg of ALT may be dosed over 120 days, although in certain cases over 7000 mg total may be administered over the 300+ day gestation period.[9]

As with all veterinary pharmaceuticals, estimating annual mass loads of ALT is complicated by the opaque nature of its production and usage. However, in the United States, it is reasonable to estimate that manufacturer-recommended doses translate to several thousand kg of annual ALT usage among ∼66 000 000 swine and 3 600 000 horses (2012 data).[10] An advertisement for Regu-Mate states that over 20 million doses were sold over its 30 years of use.[11] Although more recent comparable data does not seem to be available, ALT was easily the most widely used veterinary steroid in the United Kingdom in 2000, with 380 kg applied to the ∼10 000 000 animal swine herd.[12] For comparison, the typical annual individual dose of ethinyl estradiol for contraceptive purposes in humans is under 8 mg, with approximately ∼25 kg of ethinyl estradiol used annually in the UK.[12] Consistent with modern globalized industrial agricultural practices, additional extensive use is expected in the EU and Asia. Nevertheless, presumably because it is not a human pharmaceutical, ALT has been overlooked in recent reviews of environmental progestin pharmaceuticals,[3,13]

Although available metabolism data for ALT is incomplete and fragmented, environmental release through excretion via both urinary and fecal pathways is expected, where at least some polar metabolites exhibit reduced progestin activity.[14] In racehorses, no measurable phase I metabolites (indicating structural transformation) were observed in urine, with only phase II metabolism to glucuronide or sulfate conjugates detected.[15] In swine, the short environmental impact assessment statement for ALT indicates the excretion of several conjugated Phase II metabolites, with at least one major metabolite forming active ALT upon deconjugation and suggesting the strong possibility of glucuronide cleavage in environmental systems.[16]

There is also scant data on ALT occurrence in the environment. One study detected concentrations up to 1.1 ng/L at 4% of sites sampled in a survey of endocrine active chemicals in Minnesota lakes.[17] There is no public domain literature that documents ALT's environmental fate, to the best of our knowledge. Exposure models used in environmental impact assessments estimate concentrations below 20 ng/L in a static farm pond scenario,[16] with 0.6−9 ng/L concentrations possible in impacted receiving waters.[18] As these values fall within concentration ranges where other potent synthetic progestins impair fecundity in fish,[3,13] further investigation of ALT's environmental fate and impacts is merited.

Motivated by ALT's structural similarity to trenbolone acetate (TBA, $C_{18}H_{22}O_2$) metabolites, in the present work we evaluated ALT's photochemistry. ALT and TBA metabolites share conjugated trienone substructures, and the photochemistry of the trienone moiety controls the fate of TBA metabolites in shallow surface waters.[19−21] Specifically, direct photolysis of TBA metabolites proceeds via rapid photohydration, creating products that are not only photostable but also capable of undergoing thermal dehydration under ambient conditions.[22] These coupled processes lead to photoproduct reversion that regenerates their parent structure and would be expected to substantially increase exposure risks to TBA metabolites in affected receiving waters.[23]

For ALT, we quantified phototransformation quantum yield and evaluated the impacts of environmental factors (pH, temperature, and dissolved oxygen concentrations) on both photolysis rate and photoproduct stability. Laser flash photolysis experiments coupled with NMR spectroscopy and mass spectrometry were used to characterize major photoproducts and determine the main phototransformation mechanism. Finally, to better understand the biological implications of phototransformation products, an androgen receptor (AR)-dependent gene transcriptional activation assay (MDA-kb2 cells) and an in silico nuclear hormone receptor binding model were used to evaluate the bioactivity of ALT and its photoproducts.

EXPERIMENTAL METHODS

Photolysis Experiments and Photoproduct Characterization. Experiments used an Atlas Suntest CPS+ solar simulator equipped with a xenon lamp and an Atlas UV Suntest filter, to provide an emission spectrum (Supporting Information (SI) Figure S1) simulating that of natural sunlight at an irradiance of 250 W/m^2. Aqueous ALT solutions (10 μM, see SI for details about all reagents and materials) were prepared in deionized water from methanol stock solutions (10 mM). Direct photolysis rates were measured as a function of solution pH (3.7 to 9.5), which was adjusted using small amounts of HCl or NaOH, and temperature (30 to 44 °C). Solutions either were sparged with nitrogen or oxygen or left open to air to test the effect of variable oxygen concentration. To confirm environmental relevance, experiments were also conducted at a lower concentration (∼500 ng/L), in the presence of model organic matter (up to 80 mg/L of Fluka Humic Acid), and with commercial preparations (Regu-Mate, Matrix, and Altresyn), which contain 0.22% ALT in an oil matrix (see SI for experimental details). Quantum yield measurements and laser flash photolysis studies were also conducted as described in the SI. Aqueous ALT concentrations were measured by high performance liquid chromatography (HPLC), and NMR and mass spectrometry were used for photoproduct characterization; details of analytical methods are found in the SI.

Photoproduct Stability Determination. The possibility of product-to-parent reversion was examined by assessing photoproduct stability in the dark. ALT was photolyzed in deionized water at 30 °C, after which the temperature (4−35 °C) and pH (2−12) of the photoproduct solution was varied. The photoproduct mixture was stored in the dark, and aliquots were removed at various time points for analysis of ALT and photoproduct concentrations.

Androgen Receptor (AR)-Dependent Gene Transcriptional Activation Assay. To evaluate product bioactivity, we quantified the androgenic activity of ALT and ALT/photoproduct mixtures based on their ability to activate AR-mediated gene transcription in MDA-kb2 cells stably transformed with the pMMTV neo luc reporter gene construct.[24] Similar assessment of progesterone receptor (PR)-mediated gene transcription would have been desirable, but was beyond our capabilities. Thus, we focused on their androgenic activity because certain progestins, especially early generation synthetic progestins, are also strong AR agonists and this attribute also is implicated in their ability to disrupt endocrine function.[25] Cell culturing and transcriptional activation assays were performed following established procedures (described in SI).[24] Test solutions included dilution series of a testosterone (T)

DOI: 10.1021/acs.est.6b02608
Environ. Sci. Technol. 2016, 50, 7480−7488

standard, ALT, ALT/photoproduct mixtures, and appropriate control solutions that were reflective of solvent/media ratios in test solutions. Two ALT/photoproduct mixtures were prepared from 10 μM ALT solutions photolyzed in the Suntest solar simulator as described previously, one with significant ALT remaining (~12% of starting concentration, 40 s of photolysis) and one photolyzed until no ALT remained (9 min of photolysis), in addition to a solution photolyzed until no ALT remained and then allowed to thermally decompose in the dark for a minimum of 24 h.

In Silico Modeling of ALT and ALT Photoproduct Binding with Nuclear Hormone Receptors. To further explore conserved bioactivity in products, the potential binding of ALT and ALT photoproducts to nuclear hormone receptors was assessed via virtual docking and target screening.[26,27] Full details are provided in the SI.

RESULTS AND DISCUSSION

Direct Photolysis Rate and Quantum Yield. ALT undergoes extremely rapid direct photolysis under simulated sunlight, both at model and more environmentally relevant initial concentrations (i.e., 10 μM and 1.6 nM, respectively; see SI Figure S2). For example, in deionized water (pH 6) at 30 °C and open to air, photolysis occurred with a half-life of 27 s (k_{obs} = 2.58 ± 0.04 × 10^{-2} s^{-1}). When corrected for light screening, the quantum yield (calculated as described in the SI) was 0.38, suggesting ALT transformation is a very efficient photochemical process. Because the direct photolysis occurs so rapidly, indirect photolysis is not expected to significantly impact ALT fate in environmental systems. Further, such rapid and efficient photolysis facilitates short half-lives even in highly turbid waters with elevated dissolved organic matter concentrations (40 and 80 mg/L humic acid yielded half-lives of 6 and 10 min, respectively; see SI Figure S3), as might be expected for systems impacted by agricultural runoff.

Solution pH (from pH ~ 4–9) and temperature (~30–44 °C) were found to have no significant influence on photolysis rate constants, with half-lives of 23–28 s under all air-saturated conditions tested. Values of k_{obs} for photolysis under a range of pH, temperature, and oxygen levels are given in SI Table S1, with data used to obtain k_{obs} values from linear regression analyses shown in SI Figures S4–S6. Notably, the presence or absence of oxygen in the system had a significant effect on the ALT photolysis rate (Figure 1). At 30 °C, the reaction is half as fast ($t_{1/2}$ of 50 s, 1.38 ± 0.11 × 10^{-2} s^{-1}) when purged with O_2, and occurs almost too quickly to quantify a rate coefficient ($t_{1/2}$ of 8 s, k_{obs} of 9.1 ± 0.3 × 10^{-2} s^{-1}) when purged with N_2.

We originally hypothesized that ALT's photochemical behavior would be similar to TBA metabolites (e.g., 17β-TBOH and 17α-trenbolone (17α-TBOH)),[19] which differ from ALT in structure only at the C-17 position (see ALT structure in Figure 2 for atom numbering and ring lettering conventions). However, some major differences were observed. ALT degradation occurs far more rapidly than TBA metabolites, which typically undergo direct photolysis with half-lives approximately 2 orders of magnitude longer. Photostability of the primary photoproducts is also different. While TBA metabolites form photostable products (5- and 12-hydroxylated trenbolone variants with λ_{max} ~ 250 nm) because photohydration disrupts their conjugated trienone system, ALT photolysis (Figure 1) yields one primary photoproduct that remains photolabile. In addition, the strong dependence of ALT photolysis on oxygen concentration is not observed for

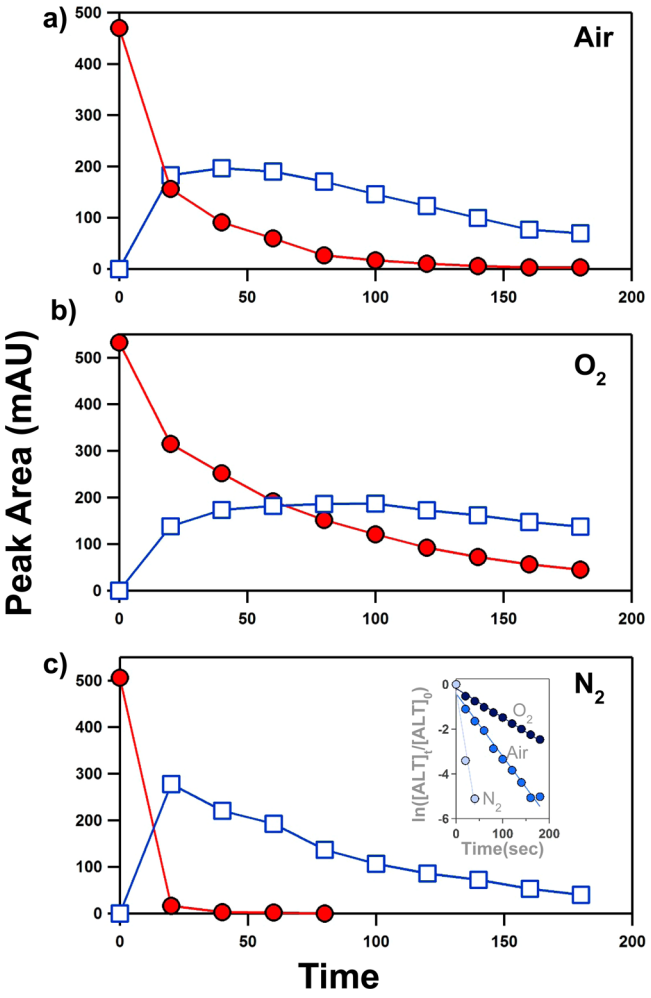

Figure 1. Direct photolysis of 10 μM ALT at pH 6 and 30 °C in deionized water left open to the air (a), purged with oxygen (b), and purged with nitrogen (c). Red circles are peak area of ALT (at 350 nm); blue hollow squares are peak area of primary photoproduct (at 320 nm). Inset on panel (c) illustrates a first order kinetic fit of the data; slopes are 9.1 ± 0.32 × 10^{-2} s^{-1} for N_2, 2.58 ± 0.04 × 10^{-2} s^{-1} for air, and 1.38 ± 0.11 × 10^{-2} s^{-1} for O_2.

TBA metabolites, and further suggests a mechanism other than a reversible photohydration for primary ALT photolysis. Of note is that photolysis of three commercial ALT preparations (all in a vegetable oil matrix) resulted in the same dominant primary photoproduct (SI Figure S7), albeit over significantly longer time scales (~2 orders of magnitude).

Primary Photoproduct Characterization. Mass spectrometry revealed that the primary photoproduct has identical mass to ALT ($[M + H]^+$ = 311.2015), suggesting isomerization. However, a significant shift in HPLC retention time (4.3 min for the primary photoproduct versus 7.0 min for ALT on a reverse-phase C18 column) and major differences in the UV–vis absorbance spectra (Figure 3a) suggest that this isomerization must produce significant structural changes. Indeed, the ^{1}H NMR spectrum of the primary photoproduct is very different from that of ALT. The vinyl region in ALT has three resonances characteristic of the endocyclic olefins in its A and C rings (δ6.55, 6.40, 5.71 ppm) and three resonances from its terminal olefin (δ5.98, 5.14, 5.10 ppm). In the photoproduct, only a single resonance remains (from the A ring olefin, δ5.60 ppm), and the alkane region increases in complexity.

DOI: 10.1021/acs.est.6b02608
Environ. Sci. Technol. 2016, 50, 7480–7488

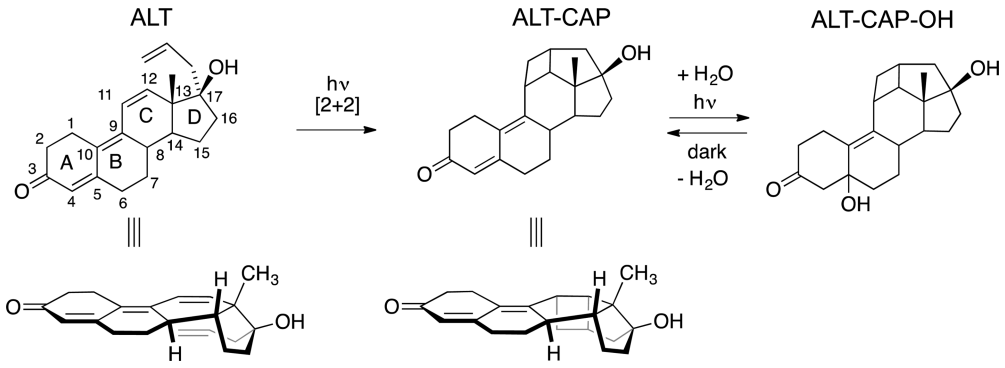

Figure 2. Proposed pathway for photolysis of ALT. Photoisomerization occurs via a 2 + 2 cycloaddition to form the primary photoproduct (ALT-CAP), which subsequently undergoes a reversible photohydration. Steroid ring lettering and atom numbering conventions are shown for ALT.

Collectively, these observations are consistent with ALT undergoing an intramolecular photochemical [2 + 2] cycloaddition reaction between the pendant alkene (C17 substituent) and the endocyclic alkene in the C ring of the steroid backbone (C11 − C12) to form new cyclobutane and cyclopentane rings in the photoproduct [hereafter altrenogest cycloaddition product (ALT-CAP), see Figure 2]. Although concerted [2 + 2] cycloaddition reactions are thermally forbidden by the Woodward−Hoffmann rules, photochemical [2 + 2] cycloadditions are allowed and have been observed in many systems since their discovery in 1908.[28]

Subsequent NMR analyses including ^{1}H, ^{13}C DEPT90 and ^{13}C DEPT135, ^{1}H−^{1}H COSY, ^{1}H−^{13}C HSQC, ^{1}H−^{13}C HMBC, and ^{1}H−^{1}H NOESY further support the formation of ALT-CAP and were used to assign all of its ^{1}H and ^{13}C signals (see SI Table S5; Table S6 includes ALT assignments for comparison). For example, the new sp^{3} CH signals at δ3.53, 2.80, 2.67, and CH_2 signals at δ3.01, 1.55 ppm show connectivity and spatial relationships consistent with the proposed formation of a cyclobutane ring via the photochemical [2 + 2] cycloaddition reaction. The HSQC data, together with the ^{13}C DEPT135, were used to establish the relationship between the CH_2 and CH carbons and their respective ^{1}H signals, and the NOESY data suggest close spatial relationships between the A, B, and E protons in the four-membered ring and the D proton in the A-ring of the molecule.

The observed shift in the UV−vis absorbance spectrum from a λ_{max} of ∼350 for ALT to a λ_{max} of ∼320 for ALT-CAP (see Figure 3a) corroborates the NMR evidence for this structural change. Woodward-Fieser rules are empirically derived and predict λ_{max} for certain classes of compounds based on structure, including α,β-unsaturated ketones such as ALT and ALT-CAP.[29,30] Both λ_{max} values agree well with those predicted by the Woodward-Fieser rules (351 for ALT, and 321 for ALT-CAP). The key difference is an additional double bond extending conjugation in the C ring for ALT compared to ALT-CAP, which according to the rules should result in a decrease in λ_{max} of 30 nm, as observed experimentally.

Laser Flash Photolysis. Fundamental insights explaining the differences in ALT (a 2 + 2 cycloaddition reaction) and 17β-TBOH (a photohydration reaction) phototransformation were obtained with laser flash photolysis (LFP) to access their triplet-state absorbance and reactivity. As shown in Figure 4a, following excitation ALT has a strong absorption around 430 nm with a lifetime (τ) of 8.4 ± 0.2 μs in N_2-purged aqueous solution. The τ decreases dramatically in the presence of O_2, a known triplet quencher, indicating that the feature is a triplet−triplet absorption; the kinetic trace of the decay is shown in SI Figure S8. Additionally, triplet energy transfer from ALT to methylene blue, a low triplet energy acceptor, was observed when 100 μM of methylene blue was present in solution.

Following excitation, 17β-TBOH has an equally strong absorption feature with a nearly identical ΔA transient absorbance spectrum to ALT (Figure 4b and SI Figure S8). This similarity is explained by both compounds sharing the same trienone chromophore; the allylic group of ALT does not substantially affect this chromophoric system (ALT and 17β-TBOH structures are both shown on Figure 4). Despite these similarities, the observed τ of 17β-TBOH was 25.5 ± 1 μs in N_2-purged solutions, a 3-fold increase over ALT. The shorter lifetime for ALT results from "triplet quenching" via the intramolecular cycloaddition reaction. Assuming that the τ of ALT and 17β-TBOH would be the same in the absence of ALT's C17 allylic group, we can use the difference in lifetime to estimate the rate of the intramolecular reaction:

$$k_A = k_T + k_I \quad (2)$$

where k_A and k_T are $1/\tau$ for ALT and 17β-TBOH, respectively, and k_I is the first-order rate of the intramolecular reaction in ALT. Using eq 2 we calculated a rate constant of 8×10^4 s^{-1}, which falls in the same range of other similar photoinduced intramolecular reactions.[31]

Secondary Photoproduct Characterization and Effects of Solution Conditions. As mentioned previously, ALT-CAP can be further photolyzed ($t_{1/2}$ ∼ 40 s, k_{obs} ∼ 2×10^{-2} s^{-1}) because its absorbance spectrum significantly overlaps the solar spectrum. One dominant photoproduct is observed during ALT-CAP photolysis, and mass spectrometry reveals that this ALT-CAP photoproduct (thus a secondary photoproduct of ALT) results from ALT-CAP photohydration ([M + H]$^{+}$ = 327.1963 Da, hereafter referred to as ALT-CAP−OH). Like photoproducts of TBA metabolites, this photohydration is reversible; ALT-CAP−OH reverts to ALT-CAP over ∼48 h in the dark (Figure 3b). This coupled photohydration-thermal dehydration sequence can be repeated over multiple light-dark cycles, and the extent of reversion appears independent of photoperiod. Although 3−4 min photoperiods are shown in Figure 3b, similar extents of reversion were observed for much longer (e.g., 8 h) photoperiods.

Temperature-dependent studies of the dark (thermal) stability of ALT-CAP−OH revealed that the rate of ALT-CAP regrowth (i.e., reversion) increases with increasing temperature (Figure 5a). The inset of Figure 5a shows Arrhenius plots for 17α-TBOH and ALT-CAP. It illustrates

DOI: 10.1021/acs.est.6b02608
Environ. Sci. Technol. 2016, 50, 7480−7488

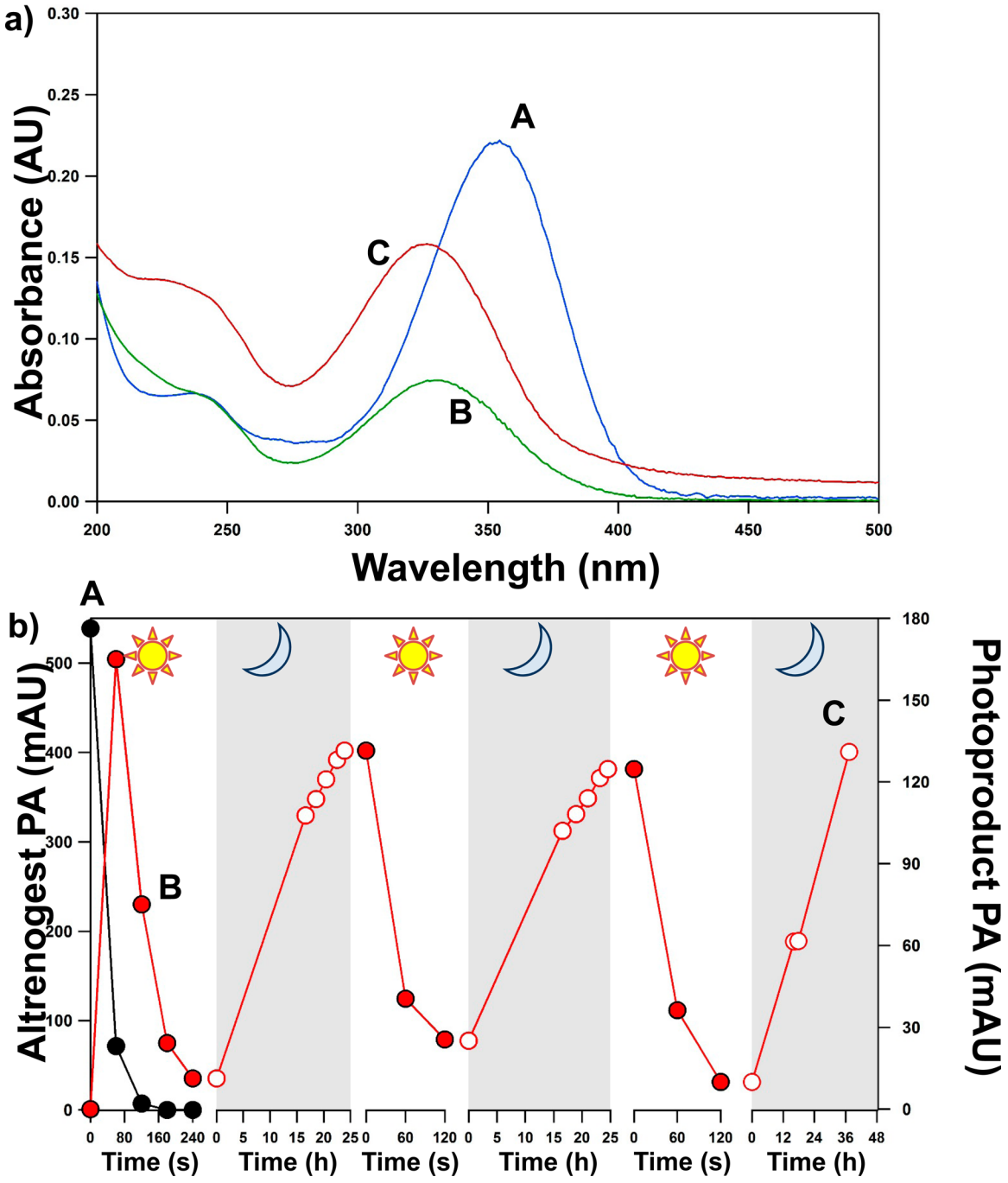

Figure 3. (a) Absorbance spectra for a 10 μM ALT solution. A (blue) is an unphotolyzed solution. B (green) has been photolyzed for 120 s and contains a mixture of primary photoproduct and ALT. C (red) has gone through multiple photolysis/dark reversion cycles and has only primary photoproduct. (b) Photolysis/dark reversion cycling of the same 10 μM ALT solution. The spectra on panel (a) correspond to points A, B, and C. Black circles are ALT (peak areas at 354 nm, primary x-axis), red circles are primary photoproduct (peak areas at 320 nm, secondary x-axis). Photolysis times are in seconds; reversion times are in hours.

that even though the absolute rate of ALT-CAP−OH dehydration is at least twice that of the major 17α-TBOH photohydrate (i.e., 5-OH-17α-TBOH),[21] the activation energies for dehydration of both species are similar (~70 kJ/mol). We interpret this near identical effect of temperature on 17α-TBOH and ALT-CAP reversion as evidence of structural similarity for their photohydrates.

Generally, pH-dependent trends in ALT-CAP−OH dehydration also mirror those for TBA metabolite photohydrates, although once again these rates are consistently faster for ALT-CAP−OH. Dehydration is acid- and base-catalyzed, occurring faster at pH 5 and 9, respectively, relative to neutral pH (Figure 5b). In fact, when ALT-CAP-OH solutions are adjusted to pH 2 or 12 immediately after their photoproduction, ALT-CAP regrowth is nearly instantaneous (SI Figure S9).

This behavior closely resembles that previously reported for 17α-TBOH, which also undergoes appreciable reversion at all pH values, whereas extensive reversion of 17β-TBOH only occurs at acidic pH values (e.g., pH 5) (see inset of Figure 5b). As we have recently detailed,[22] the greater propensity for 17α-

DOI: 10.1021/acs.est.6b02608
Environ. Sci. Technol. 2016, 50, 7480−7488

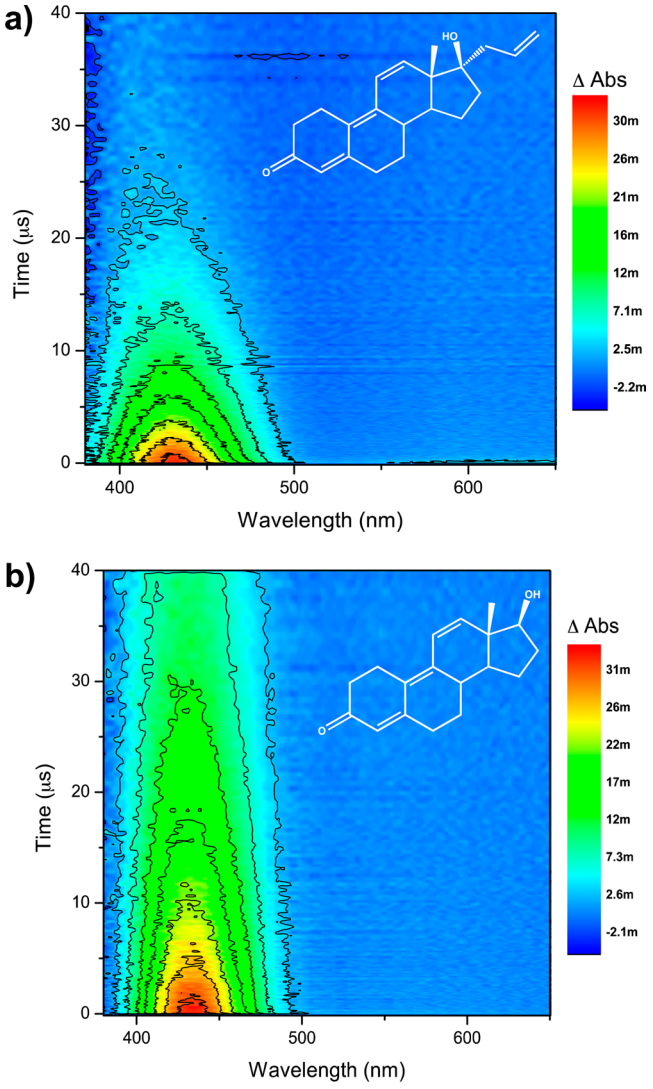

Figure 4. 2-D contour plots of transient absorption data after excitation for 100 μM solutions of ALT (a) and 17β-TBOH (b). The color scale represents transient absorption (ΔAbs) intensity.

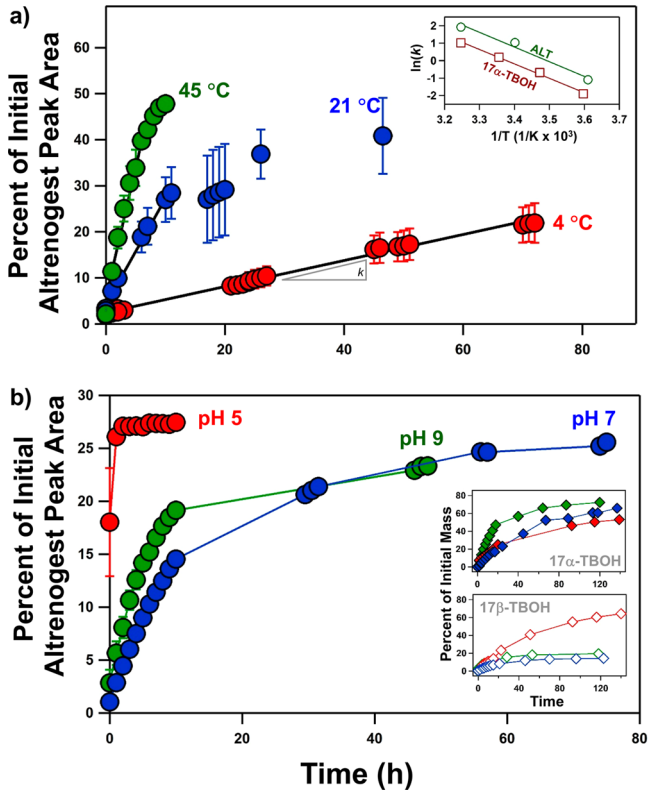

Figure 5. (a) Dependence on temperature of primary photoproduct (ALT-CAP) regeneration due to thermal decomposition of secondary photoproducts (photohydrates). ALT-CAP peak area (at 320 nm) is shown as percent of initial ALT peak area (at 354 nm). Inset shows Arrhenius plots for ALT-CAP and 17α−TBOH regeneration rates. (b) Dependence on pH of ALT-CAP regeneration from thermal decomposition of secondary photoproducts. Inset shows analogous data (red = pH 5, blue = pH 7, green = pH 9) for regeneration of 17α−TBOH and 17β−TBOH..

TBOH reversion can be attributed to its major photohydrate forming via incorporation of H^+ at C4 and OH^- at C5. In contrast, the major photohydrate of 17β-TBOH incorporates H^+ at C4 and OH^- at C12. Dehydration via water loss across C4 and C5 occurs much more quickly relative to other possible photohydrate reactions (e.g., subsequent hydration reactions) such that regeneration of 17α-TBOH can occur at all pH values.

We interpret the shared pH- and temperature dependent trends for reversion of ALT-CAP and 17α-TBOH as evidence that ALT-CAP photohydration also occurs via water addition across the C4−C5 π-bond within its dienone moiety (see Figure 2). This is logical as the 2 + 2 cycloaddition eliminates the C11−C12 π-bond such that the alternate photohydration site observed for 17β-TBOH is no longer available. Further, as with TBA metabolite photohydrates,[22] we presume that acid-catalyzed dehydration of ALT-CAP−OH occurs via a unimolecular elimination reaction (E1), where loss of water yields a resonance-stabilized carbocation intermediate that ultimately deprotonates to regenerate ALT-CAP. At higher pH, dehydration most likely proceeds via enolate formation.

Androgenic Activity of ALT and ALT Photoproducts. Androgenic activity of several synthetic progestins has been widely documented.[25,32] For example, while such data is generally limited for ALT, McRobb et al. used a yeast-based assay and determined that ALT was six times more potent than testosterone (T) and its relative potency exceeded that of 17β-TBOH.[33] In our bioassays, ALT was androgenic at a level that was eight times less potent than T; EC_{50} values for T and ALT were 0.37 and 2.9 nmol/L respectively (SI Figure S10, Table S3). 2-hydroxyflutamide extinguished androgenic activity of ALT, indicating that observed activity was AR- and not GR-mediated (data not shown). While estimates of androgenic potency were lower in the current study than those reported by McRobb et al., both indicate that ALT is an effective androgen. Potency estimate discrepancies between yeast and mammalian cell assays are common and expected; the causes of high variation between assays are addressed extensively elsewhere.[34]

Androgenic activity was also detected in the photolyzed ALT samples after 40 s of photolysis (peak of ALT-CAP formation, some ALT still present), 9 min of photolysis (ALT and ALT-CAP completely transformed), and photolysis followed by 24 h of thermal decomposition (ALT-CAP regenerated, no ALT present); see Figure 6. We emphasize that only the 40 s photolysis sample contained detectable ALT (see SI Table S2) indicating that photoproducts, and not ALT, were responsible for induction of androgenic activity in the other two samples.

DOI: 10.1021/acs.est.6b02608
Environ. Sci. Technol. 2016, 50, 7480−7488

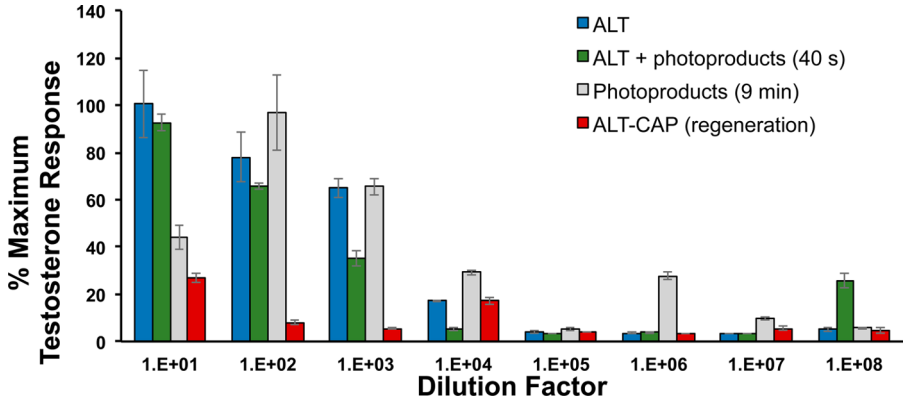

Figure 6. Androgenic activity (expressed as a percent of maximum T response) of unphotolyzed and photolyzed samples of a 10 μM ALT solution. Samples include ALT, a mixture of ALT and its photoproducts (40s, 0.12 μM ALT remaining), photoproducts only after 9 min of photolysis, and primary photoproduct only (solution photolyzed until no ALT remained and then allowed to thermally decompose in the dark for a minimum of 24 h.) All samples were serially diluted (10-fold each time) in assay media.

Highly accurate estimation of relative potency of photoproducts in comparison to ALT or the T standard is confounded by the change in concentrations over the course of the assay; ALT-CAP−OH secondary photoproducts present at the beginning of the assay undergo thermal dehydration and revert to ALT-CAP over the course of the assay (18 h, 37 °C). Furthermore, complex matrices and chemical mixtures can hinder the ability to derive definitive, high-quality estimates of androgenic potency in cell-based in vitro systems.[35] Nevertheless, our data indicate that ALT photoproducts exert significant androgenic activity. In fact, the product suite collectively exhibits activity comparable to ALT. For example, if all of the activity observed in the 9 min photolysis sample is attributed to ALT-CAP, an EC_{50} value of 0.43 nmol/L is calculated (SI Figure S10, Table S3). If this value were accurate, ALT-CAP would be a slightly less potent androgen than T and slightly more potent than ALT. However, the observation that the regeneration sample, which contains only ALT-CAP, results in a significantly lower response (maximum response was too low for EC_{50} calculation, data not included on SI Figure S10), suggests an overestimation of ALT-CAP activity due to experimental uncertainty and/or activity actually attributable to secondary photoproducts.

As a final line of evidence for conserved bioactivity through ALT phototransformation, we also employed in silico virtual target screening methods based upon three-dimensional receptor docking models. These in silico results are consistent with the aforementioned in vitro bioassays, demonstrating that ALT is predicted to have a very high binding affinity (pK_d = 8.5, or K_d = 3.2 nM) for the androgen receptor (SI Table S4). This predicted AR affinity of ALT is on par with its predicted (and expected) progesterone receptor binding (pK_d = 9.4 with a confidence interval of 1.2 pK_d units). For ALT-CAP, outcomes of in silico modeling were also in agreement with in vitro bioassay results. Specifically, virtual ligand screening data predict increased androgen receptor affinity (pK_d = 9.4) for ALT-CAP relative to ALT. Moreover, ALT-CAP also is predicted to exhibit substantial retained affinity (pK_d = 7.8) for the progesterone receptor, although this outcome requires validation with in vitro assays targeting this receptor. Based on the estimated confidence intervals of around one pK_d unit for these predictions (corresponding to an order of magnitude difference in the binding constant), the differences in pK_d values around or over 1 (e.g., 7.8 versus 9.4) are statistically significant.

Environmental Implications. These data demonstrate that assessment of risks associated with ALT occurrence in sunlit aquatic environments needs to include ALT-CAP and the secondary photoproducts. Across all tested conditions, including pH (3.7−9.5), temperature (30 to 44 °C), environmentally relevant (nanomolar) ALT concentrations, and high levels of natural organic matter (up to 80 mg/L), ALT direct photolysis was efficient and rapid. Thus, we argue it is not surprising that ALT is rarely observed in the environment. Given its very rapid photolysis rate, ALT should be expected to degrade quickly and not be at all persistent, potentially even over the time scales associated with drug handling and administration (notably, commercial formulations of ALT provide no warning on their labels about its photochemical sensitivity). The ALT photoproducts exhibit very efficient light/dark cycling, and at least some of these transformation products exhibit biological activity at picomolar to nanomolar concentrations, which is within the range anticipated to be present in agriculturally impacted receiving waters.[18] The nearly complete conservation of ALT-CAP mass through repeated photohydration-dehydration cycles is notable. This suggests that ALT-CAP-OH, unlike TBA metabolite photohydrates, is otherwise stable across all pH values and does not undergo subsequent reactions to higher order hydrated products. Thus, other fate pathways (e.g., indirect photolysis, biodegradation, sorption) will ultimately be required for attenuation of ALT-CAP mass from ALT-impacted receiving waters.

Another noteworthy finding was the high androgenic potency of ALT and clear androgenic activity of its more persistent photoproducts. These observations, along with the likely co-occurrence of ALT and ALT photoproducts with other natural and synthetic androgens in waters impacted by animal agriculture, suggest a more complex and nuanced interpretation of environmental occurrence and associated ecological hazards for these agricultural pharmaceuticals is necessary. Accordingly, future studies are needed to look for the presence of these transformation products of potential concern, especially those such as ALT-CAP, in addition to studies that will build upon these aqueous solution studies to understand more fully what will happen to these molecules in more complex matrices. These represent clear examples of what we have termed "environmental designer drugs",[35] transformation

DOI: 10.1021/acs.est.6b02608
Environ. Sci. Technol. 2016, 50, 7480−7488

products arising from environmental processes that retain substantial structure and conserved bioactivity, yet are otherwise invisible to standard, highly selective analytical methodologies focused on detection of parent compounds.

■ ASSOCIATED CONTENT

Supporting Information

The Supporting Information is available free of charge on the ACS Publications website at DOI: 10.1021/acs.est.6b02608.

Supplementary text (Materials, Altrenogest Photolysis at Environmentally Relevant Concentrations, Altrenogest Photolysis with Humic Acid, Photolysis of Commercial Oil Solutions, Quantum Yield Measurements, Laser Flash Photolysis, Analytical Methods, AR Assay Methods, In Silico Modeling of ALT and ALT Photoproduct Binding with Nuclear Hormone Receptors, Quantum Yield Calculation); solar simulator spectral output (Figure S1); ALT photolysis at low concentration and in the presence of humic acid (Figures S2 and S3), direct photolysis rate constants and data used to obtain rate constants (Table S1, Figures S4, S5, and S6); example chromatograms in water and oil matrices (Figure S7), kinetic traces of triplet state decay (Figure S8), ALT-CAP regeneration at pH 2 and 12 (Figure S9), ALT and ALT-CAP concentrations for AR assay (Table S2), dose−response curves for AR assay (Figure S10), calculated EC_{50} values (Table S3), results of in silico virtual docking and target screening (Table S4), and NMR shifts and assignments (Tables S5, S6) (PDF)

■ AUTHOR INFORMATION

Corresponding Author

*Phone: +1-651-962-5574; fax +1-651-962-5201; e-mail: khwammer@stthomas.edu.

Present Address

◆(S.K.) Department of Chemistry, Reed College, Portland, OR 97202.

Notes

The authors declare no competing financial interest.

■ ACKNOWLEDGMENTS

We thank Mr. Nicholas Cipoletti, Ms. Abigail Lukowicz, and Dr. Rachel Lundeen for assistance with data collection, Dr. Dwight Stoll with assistance in method development for oil extraction, and Dr. Kirk Heisterkamp, DVM, for assistance with acquisition of Regu-Mate® and Altresyn®. Funding support was provided by the National Science Foundation (CBET-1335711 and CBET- 1336165) and the University of St. Thomas Grants and Research Office.

■ REFERENCES

(1) Zeilinger, J.; Steger-Hartmann, T.; Maser, E.; Goller, S.; Vonk, R.; Länge, R. Effects of synthetic gestagens on fish reproduction. *Environ. Toxicol. Chem.* **2009**, *28* (12), 2663−2670.

(2) Säfholm, M.; Ribbenstedt, A.; Fick, J.; Berg, C. Risks of hormonally active pharmaceuticals to amphibians: a growing concern regarding progestagens. *Philos. Trans. R. Soc., B* **2014**, *369*, 20130577.

(3) Kumar, V.; Johnson, A. C.; Trubiroha, A.; Tumova, J.; Ihara, M.; Grabic, R.; Kloas, W.; Tanaka, H.; Kroupova, H. K. The challenge presented by progestins in ecotoxicological research: A critical review. *Environ. Sci. Technol.* **2015**, *49*, 2625−2638.

(4) Squires, E. L.; Heesemann, C. P.; Webel, S. K.; Shideler, R. K.; Voss, J. L. Relationship of altrenogest to ovarian activity, hormone concentrations and fertility of mares. *J. Anim. Sci.* **1983**, *56*, 901−910.

(5) van Leeuwen, J. J. J.; Williams, S. I.; Martens, M. R. T. M.; Jourquin, J.; Driancourt, M. A.; Kemp, B.; Soede, N. M. The effect of postweaning altrenogest treatments of primiparous sows on follicular development, pregnancy rates, and litter sizes. *J. Anim. Sci.* **2011**, *89*, 397−403.

(6) Willmann, C.; Schuler, G.; Hoffmann, B.; Parvizi, N.; Aurich, C. Effects of age and altrenogest treatment on conceptus development and secretion of LH, prosgesterone, and eCG in early-pregnant mares. *Theriogenology* **2011**, *75*, 421−428.

(7) Regu-Mate® Product label; http://www.regu-mate.com/label.asp (accessed November 9, 2015).

(8) Estienne, M. J.; Harper, A. F.; Horsley, B. R.; Estienne, C. E.; Knight, J. W. Effects of P.G. 600 on the onset of estrus and ovulation rate in gilts treated with Regu-mate. *J. Anim. Sci.* **2001**, *79*, 2757−2761.

(9) Squires, E. L. Hormonal manipulation of the mare: A review. *J. Equine Vet.Sci.* **2008**, *28*, 627−634.

(10) United States Department of Agriculture. 2012 Census of Agriculture. AC-12-A-51, 2014.

(11) Merck advertisement, http://www.miskfortune.com/regu-mate/ (accessed November 9, 2015).

(12) Boxall, A. B. A.; Fogg, L., Blackwell, P. A., Kay, P., Pemberton, E. J. *Review of Veterinary Medicines in the Environment*, R&D Technical Report P6−012/8/TR; Environment Agency: Bristol, UK, 2002.

(13) Orlando, E. F.; Ellestad, L. E. Sources, concentrations, and exposure effects of environmental gestagens on fish and other aquatic wildlife, with an emphasis on reproduction. *Gen. Comp. Endocrinol.* **2014**, *203*, 241−249.

(14) European Medicines Agency. European public MRL assessment report (EPMAR): Altrenogest (equidae and porcine species). EMA/CVMP/487477/2011, London, UK, 2012.

(15) Lampinen-Salomonsson, M. L.; Beckman, E.; Bondesson, U.; Hedeland, M. Detection of altrenogest and its metabolites in post administration horse urine using liquid chromatography tandem mass-spectrometry − increased sensitivity by chemical derivatisation of the glucoronic acid conjugate. *J. Chromatogr. B: Anal. Technol. Biomed. Life Sci.* **2006**, *833*, 245−256.

(16) Intervet, Inc. Finding of no significant impact for MATRIX (Altrenogest) solution 0.22% for cycling gilts. Millsboro, DE 2003.

(17) *Pharmaceuticals and Endocrine Active Chemicals in Minnesota Lakes*; Document number tdr-g1−16; Minnesota Pollution Control Agency: Saint Paul, MN, 2013; http://www.pca.state.mn.us.

(18) European Medical Agency Environmental Impact Assessment, 2013; http://www.ema.europa.eu/docs/en_GB/document_library/Referrals_document/Suifertil_4_mg/WC500153356.pdf (accessed November 9, 2015).

(19) Qu, S.; Kolodziej, E. P.; Cwiertny, D. M. Phototransformation rates and mechanisms for synthetic hormone growth promoters used in animal agriculture. *Environ. Sci. Technol.* **2012**, *46*, 13202−13211.

(20) Kolodziej, E. P.; Qu, S.; Forsgren, K. L.; Long, S. A.; Gloer, J. B.; Jones, G. D.; Schlenk, D.; Baltrusaitis, J.; Cwiertny, D. M. Identification and environmental implications of phototransformation products of trenbolone acetate metabolites. *Environ. Sci. Technol.* **2013**, *47*, 5031−5041.

(21) Qu, S.; Kolodziej, E. P.; Long, S. A.; Gloer, J. B.; Patterson, E. V.; Baltrusaitis, J.; Jones, G. D.; Benchetler, P. V.; Cole, E. A.; Kimbrough, K. C.; Tarnoff, D. M. Product-to-parent reversion of trenbolone: unrecognized risks for endocrine disruption. *Science* **2013**, *342*, 347−351.

(22) Baltrusaitis, J.; Patterson, E. V.; O'Connor, M.; Qu, S.; Kolodziej, E. P.; Cwiertny, D. M. Reversible photohydration of trenbolone acetate metabolites: Mechanistic understanding of product-to-parent reversion through complementary experimental and theoretical approaches. *Environ. Sci. Technol.* **2016**, DOI: 10.1021/acs.est.5b03905.

(23) Ward, A. S.; Cwiertny, D. M.; Kolodziej, E. P.; Brehm, C. C. Coupled reversion and stream-hyporheic processes increase environ-

mental persistence of trenbolone metabolites. *Nat. Commun.* **2015**, *6*, 7067.
(24) Wilson, V. S.; Bobseine, K.; Lambright, C. R.; Gray, L. E., Jr. A novel cell line, MDA-kb2, that stably expresses an androgen- and glucocorticoid-responsive reporter for the detection of hormone receptor agonists and antagonists. *Toxicol. Sci.* **2002**, *66*, 69−81.
(25) Ellestad, L. E.; Cardon, M.; Chambers, I. G.; Farmer, J. L.; Hartig, P.; Stevens, K.; Villeneuve, D. L.; Wilson, V.; Orlando, E. F. Environmental gestagens activate fathead minnow (Pimephales promelas) nuclear progesterone and androgen receptors in vitro. *Environ. Sci. Technol.* **2014**, *48*, 8179−87.
(26) Chen, Y. C.; Totrov, M.; Abagyan, R. Docking to multiple pockets or ligand fields for screening, activity prediction and scaffold hopping. *Future Med. Chem.* **2014**, *6*, 1741−1755.
(27) McRobb, R. M.; Kufareva, I.; Abagyan, R. In silico identification and pharmacological evaluation of novel endocrine disrupting chemicals that act via the ligand-binding domain of the estrogen receptor alpha. *Toxicol. Sci.* **2014**, *141*, 188−197.
(28) Wang, Z. *Comprehensive Organic Name Reactions and Reagents*; John Wiley and Sons: Hoboken, NJ, 2010.
(29) Woodward, R. B. Structure and the Absorption Spectra of α,β-Unsaturated Ketones. *J. Am. Chem. Soc.* **1941**, *63*, 1123−1126.
(30) Fieser, L. F.; Fieser, M.; Rajagopalan, S. Absorption Spectrocsopy and the Structures of the Diosterols. *J. Org. Chem.* **1948**, *13*, 800−806.
(31) Wagner, P. J.; Nahm, K. Regiospecific intramolecular reaction of an alkene group with the benzene ring of a triplet ketone. *J. Am. Chem. Soc.* **1987**, *109*, 4404−4405.
(32) Moore, N. L.; Hickey, T. E.; Butler, L. M.; Tilley, W. D. Multiple nuclear receptor signaling pathways mediate the actions of synthetic progestins in target cells. *Mol. Cell. Endocrinol.* **2012**, *357*, 60−70.
(33) McRobb, L.; Handelsman, D. J.; Kazlauskas, R.; Wilkinson, S.; McLeod, M. D.; Heather, A. K. Structure-activity relationships of synthetic progestins in a yeast-based in vitro androgen bioassay. *J. Steroid Biochem. Mol. Biol.* **2008**, *110*, 39−47.
(34) Leusch, F. D. L.; De Jager, C.; Levi, Y.; Lim, R.; Puijker, L.; Sacher, F.; Tremblay, L. A.; Wilson, V. S.; Chapman, H. F. Comparison of five in vitro bioassays to measure estrogenic activity in environmental waters. *Environ. Sci. Technol.* **2010**, *44*, 3853−3860.
(35) Cwiertny, D. M.; Snyder, S. A.; Schlenk, D.; Kolodziej, E. P. Environmental designer drugs: When transformation may not eliminate risk. *Environ. Sci. Technol.* **2014**, *48*, 11737−11745.

DOI: 10.1021/acs.est.6b02608
Environ. Sci. Technol. 2016, 50, 7480−7488